

Fragmentation by Molecular Dynamics: The Microscopic "Big Bang"

Brad Lee Holian

Theoretical Division, Los Alamos National Laboratory, Los Alamos, New Mexico 87545

and

Dennis E. Grady

Sandia National Laboratories, Albuquerque, New Mexico 87185

(Received 18 December 1987)

We propose and test a new molecular-dynamics method to study fragmentation of condensed matter under homogeneous adiabatic expansion. Our atomistic simulations give significant insight into the nature of fragment distributions. We also find that a simple continuum model based on energy balance gives a reasonably good estimate of the average fragment mass.

PACS numbers: 05.70.Ln, 46.10.+z, 62.20.Mk

The random segmentation of a one-dimensional (1D) infinite line provides an example of a geometrical statistical theory¹ whose fragment distribution is in reasonable accord with the results of 1D dynamic fragmentation experiments. Unfortunately, in more dimensions, numerous geometric constructions are possible, leading to widely differing distributions. Furthermore, because of inherent test complexity,¹ laboratory fragmentation experiments are not able to differentiate unambiguously among the various competing geometric statistical theories. We report the results of novel molecular-dynamics (MD) computer experiments on fragmentation, which do not suffer from the practical limitations of laboratory testing and which allow us to select the microscopically correct statistical theory. In these MD simulations, condensed matter undergoes adiabatic expansion and fragmentation. Our new MD technique invokes the classical, Euclidian-space picture of the "big bang," where our infinite sample (Universe) is modeled as an expanding checkerboard of periodically repeated units, each containing N atoms. Not only is this method new and interesting for its own sake, but through its use, we have been able to establish that the homogeneous distribution of fragment or cluster masses is exponential, and that the average cluster mass can be simply explained by an energy balance between the kinetic energy of expansion and the potential energy of broken surface bonds. The implications of these results are far reaching, insofar as they lend physical, albeit microscopic, credence to fragmentation models developed for a wide range of applications, from the breakup of oil shale, to the destruction of armor, and even to the distribution of galaxies in our Universe.

We first describe the MD calculations, which are meant to simulate the homogeneous expansion of an infinite system. The effects of surfaces at free boundaries are minimized by the imposition of periodic boundary conditions. Within each of the periodic units there are N particles whose initial coordinates and momenta

correspond to a specified equilibrium state of a fluid (or solid). At time zero, the side lengths of the periodic unit are made to expand at a constant (isotropic) rate: for example, in the x direction, $L_x(t) = L_x(0)(1 + \dot{\eta}t)$. This feature (other than the sign of the boundary velocity) is very much like the method for the generation of shock waves²; however, at time zero, unlike the inhomogeneous shock-wave case, a constant (homogeneous) velocity gradient is applied to all the particles within the unit. Consequently, the x velocity of particle i (coordinate x_i), for example, becomes $u_i(0+) = u_i(0) + \dot{\eta}x_i(0)$, where $\dot{\eta}$ is the initial expansion strain rate (Hubble constant in cosmological terms) and $u_i(0)$ is the initial random thermal velocity. From time zero onward, the expansion is adiabatic (no more energy is added to the system), and the particles obey Newton's equations of motion, with expanding periodic boundary conditions—that is, if an atom with coordinate x_i and velocity u_i leaves, for example, the left-hand boundary of the periodic cell, it is replaced by an image particle that enters the right-hand boundary with $x_i^* = x_i + L_x$ and $u_i^* = u_i + \dot{L}_x$.

For our atomistic simulations of expansion and fragmentation, we chose to study a 2D fluid in order to obtain a statistically significant number of fragments. For the interatomic forces, we chose the Lennard-Jones pair potential (inverse-twelfth-power repulsion and inverse-sixth-power attraction) as a realistic model potential having an attractive well. In contrast, a purely repulsive potential lacks a cohesive mechanism for clustering and therefore its phase diagram lacks a liquid-vapor coexistence dome. Moreover, the properties of the two-dimensional Lennard-Jones system are well known; for example, its phase diagram has been determined³ (see Fig. 1). The Lennard-Jones units are the atomic mass m , the distance σ at the crossing point of the pair potential, and the well-depth energy ϵ ; the unit of time is therefore $t_0 = \sigma(m/\epsilon)^{1/2}$. The interaction range of the attractive well is smoothly truncated² at $\approx 1.74\sigma$ by the fitting of a cubic spline at the inflection point, $\approx 1.24\sigma$

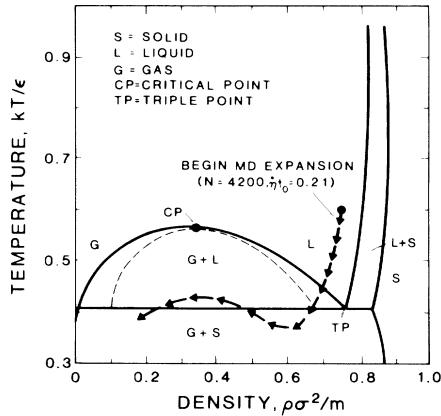


FIG. 1. Phase diagram for 2D Lennard-Jones system (Ref. 3). Arrows show MD expansion path. (Dashed curve is spinodal line.)

(the minimum of the potential is at $2^{1/6}\sigma$). We studied five subsonic expansion rates ranging in powers of two from $\eta t_0 = 0.0535$ to 0.856 ; for subsonic expansion, η must be small compared to the vibrational frequency ($72^{1/2}t_0^{-1}$ in the solid). The initial state was an equilibrium fluid at a density $\rho\sigma^2/m = 0.75$, approximately that of the triple point, and a temperature $kT/\epsilon = 0.6$, slightly higher than that of the critical point. The five experiments were terminated at a final density $\rho\sigma^2/m = 0.175$.

There are two previous studies of the 2D Lennard-Jones system that are particularly interesting in their relationship to the present work. Abraham, Koch, and Desai studied isochoric quenching into the metastable region of the vapor dome (spinodal decomposition).⁴ The principal feature of their MD simulations is the phase separation at constant temperature and density, rather than the process of fragmentation in an expanding fluid. Blink and Hoover studied the sudden heating, expansion, and fragmentation of a large 2D droplet with free boundaries.⁵ Our approach differs in its emphasis upon homogeneous expansion in the bulk fluid, *without* free boundaries, thereby facilitating comparisons with continuum theories of dynamic fragmentation.

In our MD experiments, the expanding fluid follows (approximately) an isentrope, shown as a track resembling a van der Waals loop in Fig. 1. We have computed the bulk temperature along this path from velocity fluctuations of particles about their local expansion velocity, assuming local thermodynamic equilibrium—a questionable assumption, as we point out later. Fragmentation of the bulk liquid begins somewhere near the spinodal line, where incipient cavities form due to thermal fluctuations, as seen in Fig. 2. The termination of the expansion experiment is shown in Fig. 3. This is clearly a snapshot of a nonequilibrium state, since many of the droplets are far from spherical; also, according to the kinetic temperature, only 20% of the mass should be in the condensed

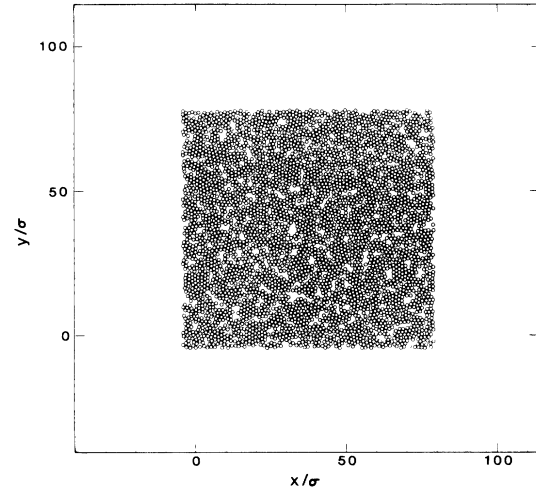


FIG. 2. Snapshot of particle positions early in 2D MD expansion ($\rho\sigma^2/m = 0.612$, $kT/\epsilon \approx 0.37$; $N = 4200$, $\eta t_0 = 0.21$, $t/t_0 = 1$).

(nonvapor) phase at equilibrium.

We have gathered cluster statistics from MD experiments at this final state for the five strain rates. The identification of clusters is done as follows: (1) Initially, each atom is considered a monomeric cluster, whose cluster number is equal to its atom number. (2) Proceeding one at a time through the list of N atoms, we make a list for each atom of its neighbors that fall within a chosen cluster bond length r_c ($\approx 1.24\sigma$), the basis for our definition of a cluster. (3) For each neighbor, we determine the larger of the two cluster numbers (the atom and its neighbor), and replace any previous occurrence in the list of clusters by the smaller number. At the end, all possible connectivities are thus accounted

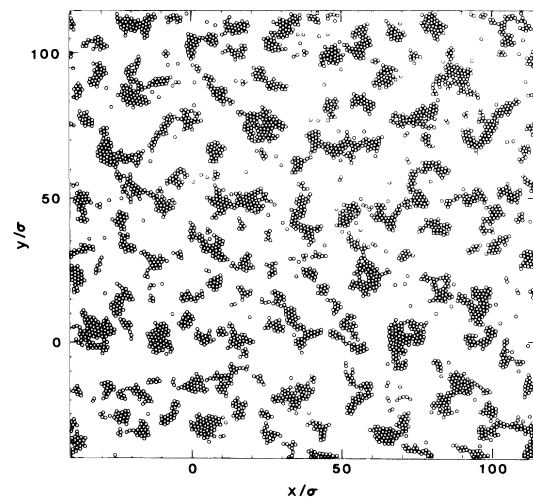


FIG. 3. Snapshot of final particle positions for 2D MD expansion experiment ($\rho\sigma^2/m = 0.175$, $kT/\epsilon \approx 0.39$; $N = 4200$, $\eta t_0 = 0.21$, $t/t_0 = 10$).

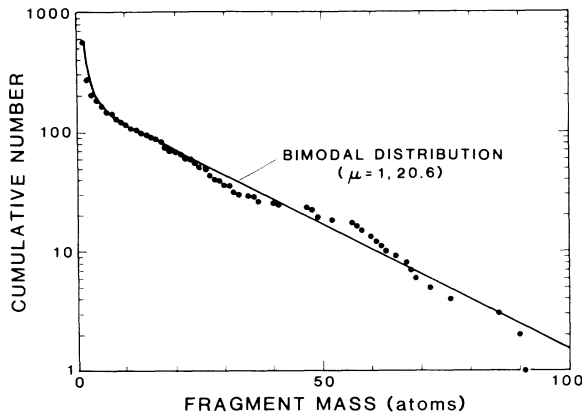


FIG. 4. Cluster statistics for the final state of 2D MD expansion ($N=4200$) at initial rate $\dot{\eta}t_0=0.21$: logarithm of cumulative number of fragments of mass M or greater (dots) vs M , along with fitted bimodal [$\Sigma \exp(-M/\mu)$] distribution (solid curve).

for. The number of atoms in each cluster is counted and the distribution of clusters is computed.

A representative fragment distribution from an MD expansion experiment is shown for the expansion rate $\dot{\eta}t_0=0.21$ in Fig. 4, where the logarithm of the cumulative number of clusters (fragments) of mass M or greater is plotted against M , in units of the atomic mass m . (The cumulative number of clusters, rather than the number itself, is reported because it is inherently less noisy, especially for large masses.) The cumulative distribution is well represented by a sum of two exponentials—a bimodal distribution; in Fig. 4, the two modes are a monomeric peak ($\mu=1$) and a broad shoulder with average fragment mass $\mu=20.6$.

An exponential fragment distribution can be derived, under the assumption of equally likely cluster masses, by our maximizing the number of ways that fragments can be distributed $N_0!/(n_1!n_2! \dots n_N!)$, where n_k is the number of clusters containing k atoms, subject to the constraints of fixed total number of atoms N and number of fragments N_0 . The derivation parallels that of maximizing the entropy to obtain the canonical Boltzmann distribution.¹ As an example of such a distribution from macroscopic experiments, Fig. 5 shows the results of exploding munitions tests of Mock and Holt, where fragments were collected after detonating explosive-filled steel cylinders.⁶ On an even larger scale, Fig. 6 shows the analysis by Brown, Karpp, and Grady of the fragmentation of the Universe by the *real* big bang, giving the distribution of galaxies as a function of absolute luminosity, considered to be proportional to galactic mass.⁷

Thus, from the atomistic to the galactic scale, homogeneous fragment distributions appear to be consistently exponential with fragment mass, rather than, as has been suggested by Mott and Linfoot, exponential with fragment diameter⁸ (or square root of mass in 2D). As

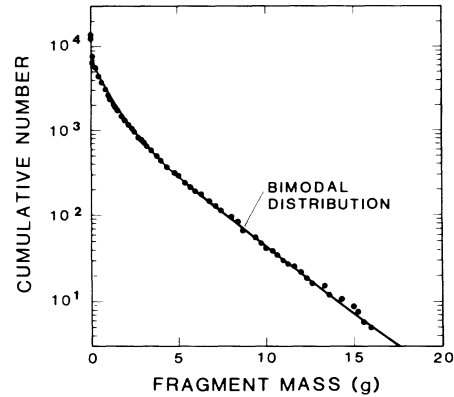


FIG. 5. Cumulative fragment number vs fragment mass for explosive fragmentation of a steel cylinder (Ref. 6).

pointed out by Grady and Kipp,¹ other geometric constructions are possible, such as the Voronoi fragmentation⁹ (which leads to a distribution that looks qualitatively like a Gaussian in fragment mass). However, the *physical* processes of fragmentation, which occur in our MD calculations, rule out these competing geometric-based theories.

It remains, then, to predict the mean or median fragment mass as a function of the initial density (perhaps temperature, too) and expansion rate, in terms of the fundamental properties of the interaction forces between atoms. Grady has proposed a simple equilibrium model, based on the balance of the kinetic energy of expansion of a spherical droplet and the potential energy required to form its surface.¹⁰ The expansion kinetic energy per unit mass is $[d/(d+2)]R^2\dot{\eta}^2/2$, where R is the radius of the d -dimensional droplet. The surface potential energy

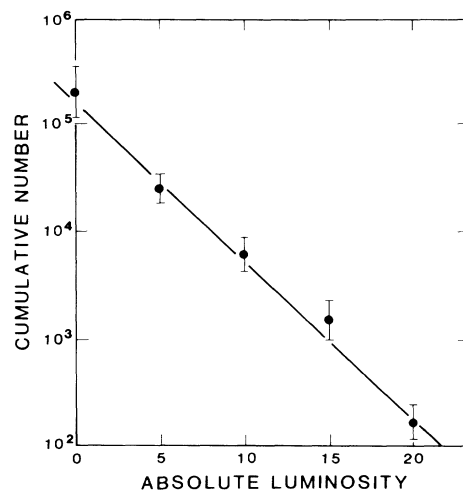


FIG. 6. Fragmentation of the Universe (Ref. 7): cumulative number of galaxies of mass M or greater, where M is assumed to be proportional to absolute luminosity (units: solar luminosity $\times 10^{10}$).

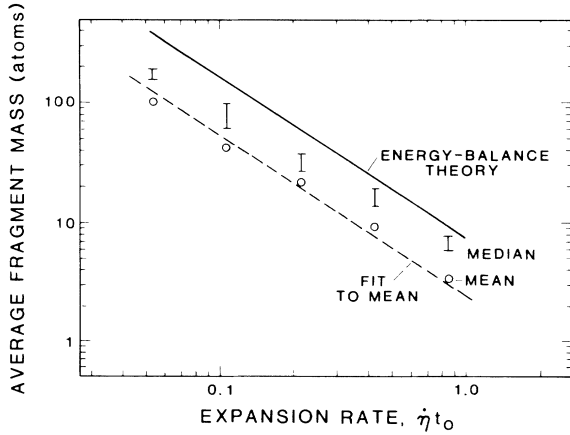


FIG. 7. Average fragment mass vs 2D MD expansion strain rate, $\dot{\eta}t_0$; $N=4200$. Both arithmetic mean and median cluster size are shown, the latter for two cluster bond-length definitions: lower end, $r_c/\sigma=1.24$; upper end, $r_c/\sigma=1.33$. Energy-balance theory (solid curve) and fit to mean cluster size (dashed curve) have slope $-\frac{4}{3}$.

per unit mass is $d(r_c/R)(E_{\text{coh}}/2)$, where E_{coh} is the cohesive energy (per unit mass) and r_c is the thickness of the shell of broken bonds. Minimization of the sum of these energy densities for the minimum surface density of a droplet gives the mean cluster mass:

$$\mu = \frac{S_d}{d} \rho \left(\frac{(d+2)r_c E_{\text{coh}}}{2\dot{\eta}^2} \right)^{d/3},$$

where $S_d = 2\pi^{d/2}/\Gamma(d/2)$ is the area of a unit d -dimensional sphere. This continuum-theory expression can be evaluated for discrete, atomistic systems in terms of the pair potential: $E_{\text{coh}} \approx n_d \epsilon / 2m$, where n_d is the number of nearest neighbors (2, 6, and 12 for $d=1, 2$, and 3, respectively), and $r_c \approx \sigma$, the range of the pair potential. For our 2D system, the mass (number of atoms) in the mean cluster is therefore $\mu \approx (0.75)6^{2/3}\pi \times (\dot{\eta}t_0)^{-4/3}$, which is shown in Fig. 7 along with the MD results for five different strain rates. In this figure, both the mean cluster mass, as determined from the slope of the broad shoulder in the log-linear plots of cumulative number versus mass (that is, excluding the monomeric

peak), and the median cluster mass (half the mass of the sample is in clusters bigger than the median) are shown. For a single exponential distribution, the median is 1.68 times the mean; for a bimodal distribution, the ratio is somewhat less. Nevertheless, this does not account for the factor of 3 by which the energy-balance theory overestimates the average cluster mass. Part of the difficulty is the fractal nature of the connectivity of clusters, as shown in Fig. 3; by a change of the cluster bond length from 1.24σ to 1.33σ , the median cluster mass increases as much as 50%. Another way of understanding this from the energetic point of view is that for the same surface area (energy), a worm-shaped cluster contains fewer atoms than a spherical cluster. As higher strain rates are achieved, the clusters become smaller and more spherical, and hence in better agreement with the simple model.

In conclusion, we have demonstrated, through the novel use of molecular dynamics, the ability to simulate realistically the fragmentation of a fluid (or solid) under homogeneous adiabatic expansion. We find that the distribution of fragment masses is exponential, in accord with information theory (maximum entropy). Moreover, a simple energy-balance theory gives a reasonably good estimate of the average fragment mass.

¹D. E. Grady and M. E. Kipp, *J. Appl. Phys.* **58**, 1210 (1985).

²B. L. Holian, *Phys. Rev. A* (to be published).

³J. A. Barker, D. Henderson, and F. F. Abraham, *Physica (Utrecht)* **106A**, 226 (1981).

⁴F. F. Abraham, S. W. Koch, and R. C. Desai, *Phys. Rev. Lett.* **49**, 923 (1982).

⁵J. A. Blink and W. G. Hoover, *Phys. Rev. A* **32**, 1027 (1985).

⁶W. Mock, Jr., and W. H. Holt, *J. Appl. Phys.* **54**, 2344 (1983).

⁷W. K. Brown, R. R. Karpp, and D. E. Grady, *Astrophys. Space Sci.* **94**, 401 (1983).

⁸N. F. Mott and E. H. Linfoot, Ministry of Supply Report No. AC3348, January, 1943 (unpublished).

⁹T. Kiang, *Astrophys.* **64**, 433 (1966).

¹⁰D. E. Grady, *J. Appl. Phys.* **53**, 322 (1982).